Chemistry of Metals and Alloys

Chem. Met. Alloys 12 (2019) 88-92
Ivan Franko National University of Lviv
www.chemetal-journal.org

Interaction of the components in the system Hf–Re–Si

Liana ZINKO[1], Oksana MATSELKO[1]*, Vasyl KORDAN[1], Galyna NYCHYPORUK[1], Roman GLADYSHEVSKII[1]

[1] *Department of Inorganic Chemistry, Ivan Franko National University of Lviv, Kyryla i Mefodiya St. 6, 79005 Lviv, Ukraine*
* *Corresponding author. Tel.:* +380-32-2394506*; e-mail: oksana.matselko@lnu.edu.ua*

Received October 25, 2019; accepted December 18, 2019; available on-line April 1, 2020
https://doi.org/10.30970/cma12.0398

The interaction of the components in the ternary system Hf–Re–Si at 1000°C has been investigated by means of X-ray powder diffraction and scanning electron microscopy with energy-dispersive X-ray spectroscopy. The system is characterized by the formation of solid solutions based on the binary phases. In addition to HfReSi and $HfReSi_2$, two more ternary phases, with approximate compositions $Hf_{23(2)}Re_{4(1)}Si_{73(1)}$ (T1) and $Hf_{71(2)}Re_{18(3)}Si_{11(1)}$ (T2), were observed. According to the EDXS analysis, the highest solubility of the third component was found for $HfRe_2$ (up to 36.4 at.% Si) and Re_4Si_7 (up to 23.8 at.% Hf). The ternary phase HfReSi exhibits a significant homogeneity range with an approximately constant Hf content at 1000°C ($Hf_{29.1(3)-25.0(4)}Re_{30.3(5)-45(2)}Si_{40.6(8)-30(2)}$).

Hafnium / Rhenium / Silicon / X-ray powder diffraction / Scanning electron microscopy

Introduction

Low thermal expansion is an important characteristic of construction materials. The peculiar properties of some of the Hf–Si and Re–Si compounds [1] make the ternary Hf–Re–Si system attractive for a detailed investigation of the interaction of the components at elevated temperatures, and the consecutive construction of isothermal sections of the phase diagram.

The systems {Ti,Zr,Hf}–{Mn,Re}–{Si,Ge,Sn,Pb}, or T^{IV}–T^{VII}–M^{IV}, have not yet been thoroughly investigated. Of the 24 ternary systems, isothermal sections of the phase diagrams (mainly partial, experimental) have been constructed only for the Ti–Mn–{Si,Ge,Sn} systems [2]. 32 ternary compounds, representing 13 structure types, 9 of them fully ordered, have been reported in the T^{IV}–T^{VII}–M^{IV} systems ([3], Table 1). It should be noted that almost all of the known compounds contain Mn and the largest number of representatives, eight, has the structure type $ZrCrSi_2$.

As for the Hf–Re–Si system in particular, two ternary compounds – HfReSi (structure type ZrNiAl, space group *P*-62*m*, Pearson symbol *hP*9) [4] and $HfReSi_2$ ($ZrCrSi_2$, *Pbam*, *oP*48) [5] – have been reported. The boundary systems, Hf–Re, Hf–Si, and Re–Si, are well known and their phase diagrams have been constructed [6]. Crystallographic parameters of the binary and ternary compounds reported prior to this investigation are summarized in Table 2.

In this work, we present the results of a preliminary investigation of the interaction of the components in the system Hf–Re–Si at 1000°C.

Experimental

Alloys were synthesized from high-purity metals (Hf ≥ 99.9 mass%, Re ≥ 99.9 mass% (pressed pellets), Si ≥ 99.999 mass%) by arc melting with a tungsten electrode, a water-cooled copper hearth and a Ti getter under argon atmosphere. After the synthesis, the ingots were sealed in quartz ampoules under vacuum, annealed at 1000°C for 1 week and quenched into cold water. Phase analysis and structure refinements were carried out using X-ray powder diffraction (XRPD) data collected on diffractometers DRON-2.0M (Fe *K*α radiation) and STOE STADI P (Cu $K\alpha_1$ radiation). The profile and structural parameters were refined by the Rietveld method, using the WinCSD program package [7]. The overall compositions of the samples and of the individual phases, in particular the solubilities of the third component in the binary phases, were investigated by means of energy-dispersive X-ray spectroscopy (EDXS; scanning electron microscope Tescan Vega 3 LMU equipped with an X-Max^{N}20 silicon drift detector).

Table 1 Structure types of known compounds in T^{IV}–T^{VII}–M^{IV} systems.

System \ Structure type		**$(Cr_{0.16}Mo_{0.38}Co_{0.46})$**, *hR*159, *R*-3	**$Nb_2Cr_4Si_5$**, *oI*44, *Ibam*	**TiFeSi**, *oI*36, *Ima*2	**$CuHf_5Sn_3$**, *hP*18, $P6_3/mcm$	**Mg_2Ni**, *hP*18, $P6_222$	**$ZrMnSi_2$**, *oI*48, *Immm*	**$CrSi_2$**, *hP*9, $P6_222$	**$Nb_3(Cr_{0.5}Fe_{0.5})_2Fe_2Si_6$**, *tP*104, $P4_2/mbc$	**$Zr_4Co_4Ge_7$**, *tI*60, *I*4/*mmm*	**TiNiSi**, *oP*12, *Pnma*	**$MgFe_6Ge_6$**, *hP*13, *P*6/*mmm*	**ZrNiAl**, *hP*9, *P*-62*m*	**ZrCrSi$_2$**, *oP*48, *Pbam*
Ti–Mn–	Si	■	■					■					■	■
	Ge			■										■
	Sn				■	■								
	Pb													
Zr–Mn–	Si						■		■	■	■			■
	Ge										■	■		■
	Sn											■		
	Pb													
Hf–Mn–	Si								■	■	■			■
	Ge											■	■	■
	Sn											■		
	Pb													
Ti–Re–	Si							■					■	
	Ge													
	Sn													
	Pb													
Zr–Re–	Si												■	■
	Ge													
	Sn													
	Pb													
Hf–Re–	Si												■	■
	Ge													
	Sn													
	Pb													
Number of representatives		**1**	**1**	**1**	**1**	**1**	**1**	**2**	**2**	**2**	**3**	**4**	**5**	**8**

Results and discussion

Twelve ternary alloys were prepared in the system Hf–Re–Si. The results of the analysis by XRPD and EDXS are summarized in Table 3; backscattered-electron (BSE) images of selected samples, together with the compositions of the identified phases, are shown on Fig. 1.

At 1000°C, the existence of the binary phases $Hf_{21}Re_{25}$, $HfRe_2$, Hf_5Re_{24}, Hf_2Si, $HfSi_2$, and Re_4Si_7, mainly in the form of ternary solid solutions, was confirmed. These findings are in agreement with the assessed binary phase diagrams [20-22]. In addition, we observed a Hf_5Si_3-based solid solution. Hf_5Si_3 exists between 1718 and 2510°C and forms *via* the peritectic reaction L + Hf_3Si_2 ↔ Hf_5Si_3 at 2510°C [23]. At first, this phase was considered to be stabilized by C, N, or O [24-26], but later it was found to be stable as a binary phase [27]. We also observed ReSi (exists between 1650-1820°C; L + $ReSi_{1.75}$ ↔ ReSi at 1820°C), while Hf_3Si_2 (L ↔ Hf_3Si_2 at 2480°C), Hf_5Si_4 (L + Hf_3Si_2 ↔ Hf_5Si_4 at 2320°C), and Re_2Si (L ↔ Re_2Si at 1810°C) were not detected.

The existence of the reported ternary phases HfReSi and $HfReSi_2$ at 1000°C was confirmed as well. In addition, two new ternary phases with approximate compositions $Hf_{23(2)}Re_{4(1)}Si_{73(1)}$ (T1) and $Hf_{71(2)}Re_{18(3)}Si_{11(1)}$ (T2) were detected.

In the region 63.6-66.7 at.% Si of the system Re–Si four compounds with close compositions have been reported: triclinic $ReSi_{1.75}$, monoclinic Re_4Si_7, tetragonal $ReSi_{1.8}$, and orthorhombic $ReSi_2$. For the Rietveld refinements, performed on multiphase samples, we used the monoclinic crystal structure model.

According to the EDXS analysis, the highest solubilities of the third component were found for $HfRe_2$ (up to 36.4 at.% Si) and Re_4Si_7 (up to 23.8 at.% Hf). The ternary phase HfReSi showed a significant homogeneity range at an almost constant Hf content ($Hf_{29.1(3)-25.0(4)}Re_{30.3(5)-45(2)}Si_{40.6(8)-30(2)}$).

Table 2 Crystallographic parameters of binary and ternary compounds in the systems Hf–Re, Hf–Si, Re–Si, Hf–Re–Si. Binary phases stable at 1000°C are highlighted.

Compound	Structure type	Pearson symbol	Space group	Unit-cell parameters, Å			Ref.
				a	*b*	*c*	
$Hf_{21}Re_{25}$	$Zr_{21}Re_{25}$	*hR*276	*R*-3*c*	25.773	–	8.760	[8]
$HfRe_2$	$MgZn_2$	*hP*12	$P6_3/mmc$	5.239	–	8.584	[9]
Hf_5Re_{24}	Ti_5Re_{24}	*cI*58	*I*-43*m*	9.708	–	–	[10]
Hf_2Si	$CuAl_2$	*tI*12	*I*4/*mcm*	6.553	–	5.186	[11]
Hf_5Si_3	Mn_5Si_3	*hP*16	$P6_3/mcm$	7.844	–	5.492	[12]
Hf_3Si_2	U_3Si_2	*tP*10	*P*4/*mbm*	6.988	–	3.675	[12]
Hf_5Si_4	Zr_5Si_4	*tP*36	$P4_12_12$	7.039	–	12.83	[12]
HfSi	FeB	*oP*8	*Pnma*	6.889	3.772	5.223	[12]
$HfSi_2$	$ZrSi_2$	*oS*12	*Cmcm*	3.672	14.57	3.641	[12]
Re_2Si	Re_2Si	*mP*24	$P2_1/c$	6.4444	9.6019 β = 94.214°	5.3898	[13]
Re_5Si_3	W_5Si_3	*tI*32	*I*4/*mcm*	9.53	–	4.81	[14]
ReSi	FeSi	*cP*8	$P2_13$	4.7744	–	–	[15]
Re_4Si_7	Re_4Si_7	*mS*44	*Cm*	23.167	3.14 β = 94.214°	8.3018	[16]
$ReSi_{1.75}$	$ReSi_{1.75}$	*aP*6	*P*1	3.12 α = 90°	3.138 β = 90.1°	7.67 γ = 90°	[17]
$ReSi_{1.8}$	$MoSi_2$	*tI*6	*I*4/*mmm*	3.132	–	7.681	[18]
$ReSi_2$	$ReSi_2$	*oI*6	*Immm*	3.128	3.144	7.677	[18]
HfReSi	ZrNiAl	*hP*9	*P*-62*m*	6.927	–	3.391	[4]
$HfReSi_2$	$ZrCrSi_2$	*oP*48	*Pbam*	9.106	10.016	8.062	[5]

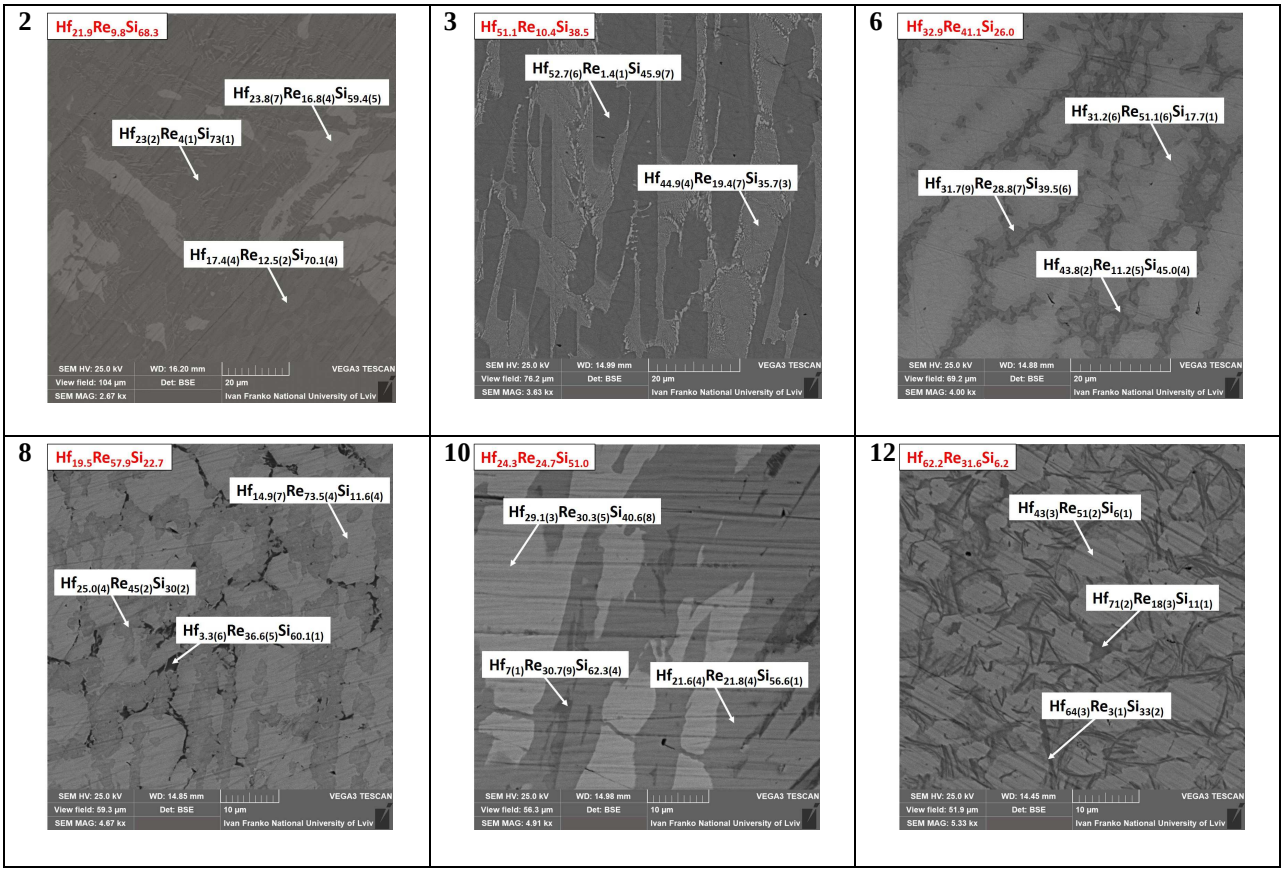

Fig. 1 Microstructures of selected samples (BSE images) and compositions of the observed phases.

Table 3 Results of the phase analysis of the synthesized samples.

Sample [a]		Phase [b]	Pearson symbol	Space group	Unit-cell parameters, Å		
					a	*b*	*c*
1	$Hf_{15}Re_{15}Si_{70}$	**Re_4Si_7**	*mS*44	*Cm*	23.1718(5)	3.13614(6) β = 92.735(3)°	8.2815(2)
		$HfSi_2$	*oS*12	*Cmcm*	3.67478(9)	14.5380(4)	3.64225(10)
		Si	*cF*8	*Fd*-3*m*	5.4237(5)	–	–
2	$Hf_{33}Re_{10}Si_{57}$ $Hf_{21.9}Re_{9.8}Si_{68.3}$	**$HfSi_2$** $Hf_{17.4(4)}Re_{12.5(2)}Si_{70.1(4)}$	*oS*12	*Cmcm*	3.6727(2)	14.5321(9)	3.6415(2)
		Re_4Si_7 $Hf_{23.8(7)}Re_{16.8(4)}Si_{59.4(5)}$	*mS*44	*Cm*	23.110(4)	3.1383(4) β = 92.79(2)°	8.294(1)
		T1 $Hf_{23(2)}Re_{4(1)}Si_{73(1)}$					
3	$Hf_{57}Re_{10}Si_{33}$ $Hf_{51.1}Re_{10.4}Si_{38.5}$	**Hf_5Si_3** $Hf_{52.7(6)}Re_{1.4(1)}Si_{45.9(7)}$	*hP*16	*P*6$_3$/*mcm*	7.819(1)	–	5.476(1)
		$HfRe_2$ $Hf_{44.9(4)}Re_{19.4(7)}Si_{35.7(3)}$	*hP*12	*P*6$_3$/*mmc*	5.222(2)	–	8.513(6)
4	$Hf_{60}Re_{20}Si_{20}$	**$Hf_{21}Re_{25}$**	*hR*276	*R*-3*c*	25.69(2)	–	8.757(8)
		Hf_2Si	*tI*12	*I*4/*mcm*	6.537(3)	–	5.219(4)
		unidentified phase					
5	$Hf_{50}Re_{30}Si_{20}$	**$HfRe_2$**	*hP*12	*P*6$_3$/*mmc*	5.226(1)	–	8.549(3)
		Hf_2Si	*tI*12	*I*4/*mcm*	6.335(2)	–	5.202(3)
		unidentified phase					
6	$Hf_{33}Re_{47}Si_{20}$ $Hf_{32.9}Re_{41.1}Si_{26.0}$	**$HfRe_2$** $Hf_{31.2(6)}Re_{51.1(6)}Si_{17.7(1)}$	*hP*12	*P*6$_3$/*mmc*	5.1899(1)	–	8.5009(3)
		HfReSi $Hf_{31.7(9)}Re_{28.8(7)}Si_{39.5(6)}$	*hP*9	*P*-62*m*	6.9205(8)	–	3.4133(7)
		HfSi $Hf_{43.8(2)}Re_{11.2(5)}Si_{45.0(4)}$	*oP8*	*Pnma*	9.902(4)	3.776(2)	5.272(3)
7	$Hf_{33}Re_{57}Si_{10}$	**$HfRe_2$**	*hP*12	*P*6$_3$/*mmc*	5.2238(6)	–	8.548(2)
8	$Hf_{20}Re_{60}Si_{20}$ $Hf_{19.5}Re_{57.9}Si_{22.7}$	**Hf_5Re_{24}** $Hf_{14.9(7)}Re_{73.5(4)}Si_{11.6(4)}$	*cI*58	*I*-43*m*	9.597(1)	–	–
		$HfRe_2$ $Hf_{3.3(6)}Re_{36.6(5)}Si_{60.1(1)}$?	*hP*12	*P*6$_3$/*mmc*	5.145(1)	–	8.418(3)
		HfReSi $Hf_{25.0(4)}Re_{45(2)}Si_{30(2)}$	*hP*9	*P*-62*m*	6.92(1)	–	3.375(6)
9	$Hf_{10}Re_{57}Si_{33}$	**Hf_5Re_{24}**	*cI*58	*I*-43*m*	9.5135(8)	–	–
		ReSi	*cP*8	*P*2$_1$3	4.7765(4)	–	–
		HfReSi	*hP*9	*P*-62*m*	6.903(3)	–	3.352(2)
10	$Hf_{25}Re_{25}Si_{50}$ $Hf_{24.3}Re_{24.7}Si_{51.0}$	**HfReSi** $Hf_{29.1(3)}Re_{30.3(5)}Si_{40.6(8)}$	*hP*9	*P*-62*m*	6.921(2)	–	3.385(2)
		$HfReSi_2$ $Hf_{21.6(4)}Re_{21.8(4)}Si_{56.6(1)}$	*oP*48	*Pbam*	9.119(3)	10.027(3)	8.064(3)
		Re_4Si_7 $Hf_{7(1)}Re_{30.7(9)}Si_{62.3(4)}$	*mS*44	*Cm*	23.2(4)	3.126(3) β = 92.7(1)°	8.28(1)
11	$Hf_{33.3}Re_{33.3}Si_{33.4}$	**HfReSi**	*hP*9	*P*-62*m*	6.9218(2)	–	3.3898(1)
		$HfRe_2$	*hP*12	*P*6$_3$/*mmc*	5.257(2)	–	8.592(5)
		unidentified phase				–	
12	$Hf_{64}Re_{29}Si_7$ $Hf_{62.2}Re_{31.6}Si_{6.2}$	**$Hf_{21}Re_{25}$** $Hf_{43(3)}Re_{51(2)}Si_{6(1)}$	*hR*276	*R*-3*c*	25.676(9)	–	8.757(5)
		Hf_2Si $Hf_{64(3)}Re_{3(1)}Si_{33(2)}$	*tI*12	*I*4/*mcm*	6.516(6)	–	5.261(9)
		T2 $Hf_{71(2)}Re_{18(3)}Si_{11(1)}$					

[a] nominal composition and overall composition according to elemental mapping (when available);
[b] phase identified by XRPD and composition according to EDXS (when available)

Conclusions

The system Hf–Re–Si at 1000°C is characterized by significant solubility of the third component in the binary phases. In addition to the already known compounds, two new ternary phases with approximate compositions $Hf_{23(2)}Re_{4(1)}Si_{73(1)}$ (T1) and $Hf_{71(2)}Re_{18(3)}Si_{11(1)}$ (T2) were observed. Their structures will be the topic of a future publication.

Acknowledgement

This work was supported by the Ministry of Education and Science of Ukraine under the grant No. 0118U003609.

References

[1] I. Engström, B. Lönnberg, *J. Appl. Phys.* 63 (1988) 4476-4484.
[2] SpringerMaterials (*https://materials.springer.com*).
[3] P. Villars, K. Cenzual (Eds.), *Pearson's Crystal Data – Crystal Structure Database for Inorganic Compounds*, Release 2017/18, ASM International, Materials Park, OH, 2017.
[4] Y.P. Yarmolyuk, E.I. Gladyshevskii, *Dopov. Akad. Nauk Ukr. RSR, Ser. B* (1974) 1030-1032.
[5] Y.P. Yarmolyuk, M. Sikiritsa, L.G. Akselrud, L.A. Lysenko, E.I. Gladyshevskii, *Sov. Phys. Crystallogr.* 27 (1982) 652-653.
[6] P. Villars, H. Okamoto, K. Cenzual (Eds.), *ASM Alloy Phase Diagram Database*, Release 2006/2018, ASM International, Materials Park, OH, 2018.
[7] L. Akselrud, Yu. Grin, *J. Appl. Crystallogr.* 47 (2014) 803-805.
[8] K. Cenzual, E. Parthé, R.M. Waterstrat, *Acta Crystallogr. C* 42 (1986) 261-266.
[9] V.B. Compton, B.T. Matthias, *Acta Crystallogr.* 12 (1959) 651-654.
[10] E.M. Savitskii, M.A. Tylkina, I.A. Tsyganova, E.I. Gladyshevskii, M.P. Mulyava, *Russ. J. Inorg. Chem.* 7 (1962) 831-832.
[11] E.E. Havinga, H. Damsma, P. Hokkeling, *J. Less-Common Met.* 27 (1972) 169-186.
[12] O.G. Karpinskii, B.A. Evseyev, *Russ. Metall.* (1969) 128-130.
[13] T. Siegrist, J.E. Greedan, J.D. Garrett, G. Wenhe, C.V. Stager, *J. Less-Common Met.* 171 (1991) 171-177.
[14] A.G. Knapton, *Plansee Proc. Pap. Plansee Semin. "de Re Met.", 3rd*, 1959, pp. 412-418.
[15] V.M. Fedyna, R.E. Gladyshevskii, *Visn. Lviv. Univ., Ser. Khim.* 55 (2014) 87-92.
[16] S. Harada, H. Hoshikawa, K. Kuwabara, K. Tanaka, E. Okunishi, H. Inui, *Philos. Mag.* 91 (2011) 3108-3127.
[17] U. Gottlieb, B. Lambert Andron, F. Nava, M. Affronte, O. Laborde, A. Rouault, R. Madar, *J. Appl. Phys.* 78 (1995) 3902-3907.
[18] J.L. Jorda, M. Ishikawa, J. Muller, *J. Less-Common Met.* 85 (1982) 27-35.
[19] T. Siegrist, F. Hulliger, G. Travaglini, *J. Less-Common Met.* 92 (1983) 119-129.
[20] T.B. Massalski (Ed.), *Binary Alloy Phase Diagrams*, Second Edition, ASM International, Materials Park, Ohio, 1990, Vol. 3, pp. 2105-2106.
[21] T.B. Massalski (Ed.), *Binary Alloy Phase Diagrams*, Second Edition, ASM International, Materials Park, Ohio, 1990, Vol. 3, pp. 2111-2112.
[22] T.B. Massalski (Ed.), *Binary Alloy Phase Diagrams*, Second Edition, ASM International, Materials Park, Ohio, 1990, Vol. 3, pp. 3204-3205.
[23] E. Brukl, *Tech. Rep. AFML-TR-65-2*, Air Force Materials Laboratory, WPAFB (OH), 1968, 72 p.
[24] A.K. Shurin, N. Todorov, *Metallofiz.* 33 (1971) 100-102.
[25] R. Kieffer, F. Benesovsky, *Powder Metall.* (1/2) (1958) 145-171.
[26] H. Nowotny, E. Laube, T. Kieffer, F. Benesovsky, *Monatsh. Chem.* 89 (1958) 701-707.
[27] B.P. Bewlay, J.A. Sutliff, R.R. Bishop, *J. Phase Equilib.* 20 (1999) 109-112.